Monazite Th-Pb age depth profiling

Marty Grove
T. Mark Harrison
Department of Earth and Space Sciences and Institute of Geophysics and Planetary Physics, University of California, Los Angeles, California 90095-1567, USA

ABSTRACT

The significant capabilities of the ion microprobe for thermochronometric investigations of geologic materials remain largely unexploited. Whereas $^{208}Pb/^{232}Th$ spot analysis allows ~10-mm-scale imaging of Pb loss profiles or overgrowths in sectioned monazite grains, the spatial resolution offered by depth profiling into the surface region of natural crystals is more than two orders of magnitude higher. We document here the ability of the high-resolution ion microprobe to detect $^{208}Pb/^{232}Th$ age differences of <1 m.y. with better than 0.05 μm depth resolution in the outer micron of Tertiary monazites from the hanging wall of the Himalayan Main Central thrust. Age gradients on this scale are inaccessible to ion microprobe spot analysis or conventional thermal ionization mass spectrometry. Interpretation of the near-surface ^{208}Pb distributions with available monazite Pb diffusion data illustrates the potential of the approach for recovering continuous, high-temperature thermal history information not previously available.

INTRODUCTION

Because the traditional goal of basement geochronology is to determine rock formation ages, dating methods based upon daughter products of radioactive decay that are not completely retained within mineral hosts under crustal conditions failed in this role. However, the recognition that the inhomogeneous distribution of daughter product produced by diffusion in comparatively unretentive phases can provide a rich record of paleotemperature variation with time has significantly expanded the focus of radiometric age dating (Dodson, 1973). Until recently, such thermal history analysis has largely been the domain of the K-Ar and fission-track dating methods, which has restricted its applicability to temperatures less than about 500 °C (McDougall and Harrison, 1988). With the advent of U-Pb ion microprobe dating of accessory minerals (Compston et al., 1984), it has become possible to routinely resolve age variation down to the ~10 μm scale using spot analysis (e.g., Harrison et al., 1999). Because the technique involves ion drilling into the sample, it intrinsically measures variation in isotope ratios as a function of crater depth (Ireland, 1995). Use of such information in geochronology has thus far been limited to detecting metamorphic overgrowths in zircon (Zeitler et al., 1989). However, available Pb diffusion data (Smith and Giletti, 1997) indicate that significant age variations can be expected near the margins of monazite following protracted cooling or transient heating. By forward modeling age profiles from the outer several microns of monazite using appropriate solutions to the diffusion equation (Dodson, 1973), it should be possible to obtain continuous thermal histories extending from well above 600 °C to about 400 °C (Smith and Giletti, 1997). We have developed a method to determine precise $^{208}Pb/^{232}Th$ age profiles in the near-surface region of monazite crystals as young as 5 Ma with a depth resolution of better than 0.05 μm. This method was applied to a hanging wall of the Main Central thrust in the central Himalaya with the goal of recovering thermal history information related to its displacement history.

EXPERIMENTAL APPROACH

Specimen DH-68-96 was obtained from a posttectonic granite pegmatite dike in the Darondi Khola, central Nepal, that was intruded into hanging-wall gneisses of the Main Central thrust. The sampled location is 100–200 m structurally above the mapped position of the thrust (Colchen et al., 1986). Existing thermochronologic data indicate that the hanging-wall rocks were exhumed from ~20 km depths during the late Miocene and Pliocene (8–3 Ma) by renewed thrusting in the shear zone beneath the Main Central thrust (Harrison et al., 1997, 1998). Tabular monazites exhibiting morphologies consistent with preservation of primary crystal faces were hand-selected from a heavy mineral concentrate. Grain dimensions parallel to {100} varied between 100 and 250 μm; those normal to this face were roughly half this distance. The tabular {100} faces of crystals were press mounted onto an adhesive substrate together with similarly oriented 554 standard monazite (45 ± 1 Ma; Harrison et al., 1999). A second set of 554 grains embedded in a previously polished and trimmed epoxy mount was positioned adjacent to the individually mounted grains so that the effects of using polished and unpolished grains on the calibration procedure could be gauged. Additional epoxy was poured to form a composite mount, which was then ultrasonically cleaned in ethanol and Au coated to a thickness of ~50 A without further polishing. This procedure generally resulted in adequate exposure of unpolished grains. After age depth profiling measurements had been completed, the composite mount was polished to a depth of ~10 μm to permit conventional spot analysis of DH-68-96 grains.

Details of analytical protocols for $^{208}Pb/^{232}Th$ dating of monazite using the CAMECA ims 1270 ion microprobe were given in Harrison et al. (1995, 1999). To summarize, a mass resolving power of 4500 adequately separates all molecular interferences in the 204–208 mass range. The Pb/Th relative sensitivity factor required to calculate a Th-Pb age from isotope data obtained from an unknown is determined by referring the ThO_2^+/Th^+ determined in the analysis to a calibration curve that is constructed from measurements of ThO_2^+/Th^+ vs. Pb^+/Th^+ from 554 standard monazite. The appreciable (typically 3%–8%) Th concentrations in monazite (Montel, 1993) and ~1% ionization efficiency for Pb under O^- bombardment are sufficiently favorable that the precision of $^{208}Pb/^{232}Th$ age determinations of samples older than ca. 5 Ma is limited by the reproducibility of the calibration curve (typically ±2%; Harrison et al., 1995, 1999). Data from both polished and unpolished 554 monazite were regressed together to define the calibration line used to reduce results from DH-68-96 monazite. As shown in Figure 1, results obtained from the outer 0.1 μm of unpolished 554 monazite deviates significantly from the calibration line.

Data Repository item 9940 contains additional material related to this article.

Although this behavior may in part be an artifact of surface contamination, it occurred in spite of our use of an aperture to block secondary ions emitted from periphery of the analysis area. Because this action significantly reduced common Pb but had little effect upon the initial discrepancy in the calibration data, we believe the initial discordance primarily reflects near-surface Pb loss in 554 monazite.

Pit dimensions formed in unpolished 554 monazite with a 25-mm-diameter, O^- primary beam were measured with a surface profilometer with a nominal precision of ±0.005 μm (Fig. 2A). As shown in Figure 2A, we limited the depth/diameter ratio of the sputtered craters to <0.1 to minimize variations in the sputtering conditions at the sample surface. Measuring the excavation depth as a function of time in unpolished 554 yielded a 1.44 ± 0.03 μm/hr sputter rate for a primary beam intensity of 4 nA O^- (Fig. 2B; see Table 1[1]). Crater depths corresponding to the time of individual ^{208}Pb measurements were calculated from this relationship after normalizing for drift in primary beam current and allowing for the duration of initial sputtering prior to analysis (Table 1 [see footnote 1]). Most depth profiling experiments lasted 1 hr, whereas initial sputtering to remove the Au coat and perform peak centering was 2–3 min. Measurement of the primary beam current both before and after analysis indicated that drift was generally <1%/hr. Corrections for common ^{208}Pb used to calculate ^{232}Th-^{208}Pb ages were based upon the ^{207}Pb correction procedure (see Compston et al., 1984) using the composition of common Pb (^{208}Pb/^{207}Pb = 2.50 ± 0.01) measured in Tertiary Himalayan leucogranites (Vidal et al., 1982; Schärer et al., 1986). Because ^{204}Pb signals are typically close to background levels whereas ^{207}Pb intensities are at least a factor of five higher, this approach yields results that are equivalent in effect, but more precise than, those obtained using ^{204}Pb as a proxy for common Pb.

[1]Data Repository item 9940, Tables 1–3, are available on request from Document Secretary, GSA, P.O. Box 9140, Boulder, CO 80301, editing@geosociety.org, or at www.geosociety.org/pubs/drpint.htm.

RESULTS

Depth profiling analysis of unpolished 554 monazite revealed monotonically increasing ages from 38 to 45 Ma over the first 0.15 μm and homogeneous ages thereafter (Fig. 3A). Such relatively minor near-surface depletion of ^{208}Pb in 554 monazite (Fig. 3A) is consistent with diffusive loss during protracted residence at ~15 km depths (Anderson et al., 1988). In contrast, ^{208}Pb/^{232}Th age gradients measured from the outer 0.3 μm of unpolished DH-68-96 (Fig. 3B) represent more than 50% variation in the age of the specimen (Table 2 [see footnote 1]). We emphasize that depth profiling analysis of conventionally polished grains of either standard monazite 554 or DH-68-96 produced no resolvable near-surface age variation (Fig. 3; Table 3 [see footnote 1]). Dashed lines in Figure 3B correspond to ages calculated assuming common ^{208}Pb/^{207}Pb = 2.7 (lower bound) and ^{208}Pb/^{207}Pb = 2.3 (upper bound). As indicated, low radiogenic ^{208}Pb (^{208}Pb*) yields near the grain surface (between 0% and 80% radiogenic assuming common ^{208}Pb/^{207}Pb = 2.5) cause ages measured from this region to be sensitive to the magnitude of the correction for common Pb. The ^{208}Pb/^{232}Th ages obtained in the initial 0.05 μm beneath the surface tend to be younger than ^{40}Ar/^{39}Ar mica ages from the Darondi Khola (Copeland et al., 1991), and in some cases are even negative. Because the predicted closure temperature of Pb in monazite for this length scale (~400 °C, Smith and Giletti, 1997) is slightly higher than that for Ar in micas (McDougall and Harrison, 1988), this indicates that we have overcorrected for common ^{208}Pb. We emphasize that while results from the outer

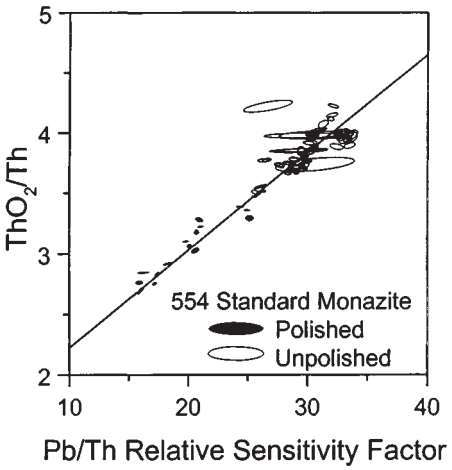

Figure 1. Th-Pb calibration (see Harrison et al., 1995) results from polished and unpolished 554 standard monazite. Although results from unpolished samples are displaced to higher ThO_2/Th values relative to those from polished 554, both are well described by same calibration line. Error ellipses represent 1σ uncertainties.

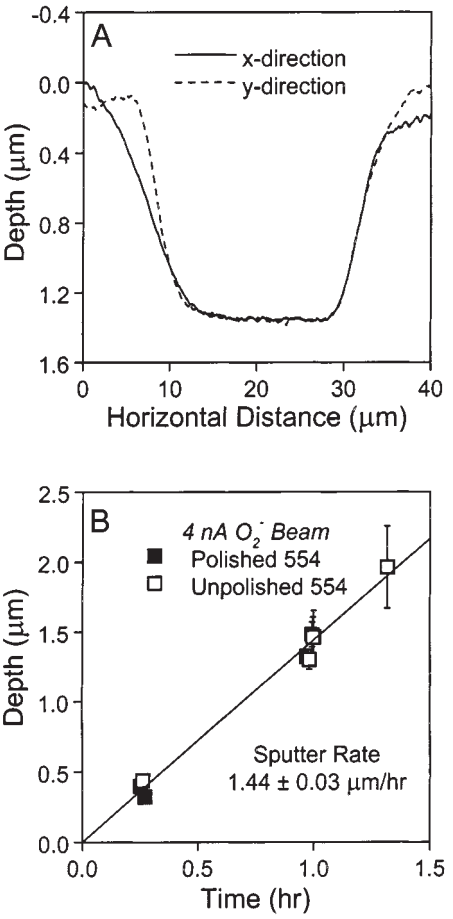

Figure 2. A: Mutually orthogonal profilometer scans across representative pit formed in unpolished 554 monazite after 1 hr sputtering duration. B: Calibration of sputtering rate. Depths for individual runs in Table 1 (see text footnote 1) were normalized to 4 nA primary current prior to regression.

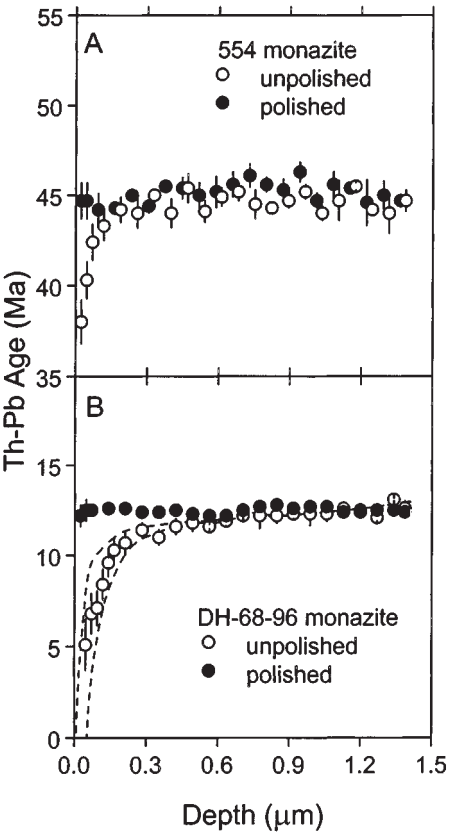

Figure 3. A: Representative Th-Pb age depth-profiling results for near-surface (unpolished) and internal (polished) regions of 554 standard monazite. B: Same for DH-68-96 monazite. Dashed lines show age variation caused by varying ^{208}Pb/^{207}Pb in common lead correction from 2.7 (lower bound) to 2.3 (upper bound).

0.05 μm are problematic, Pb contamination contributed by the epoxy and/or gold coat is not obviously the cause. Specifically, the $^{208}Pb/^{207}Pb$ ratio of material sputtered from Au-coated, unpolished epoxy (2.55 ± 0.07) is virtually identical to the value determined for Himalayan leucogranites that we have used to estimate common Pb in DH-68-96 (Vidal et al., 1982; Schärer et al., 1986).

To ascertain the tectonic significance of age profiles measured from the outer margin of DH-68-96 monazites, we have assumed uniform Th concentrations and adapted appropriate solutions of the diffusion equation (see equation A9 in Lovera et al., 1989) to predict radial distribution of ^{208}Pb as a function of thermal history. A single diffusion domain model with Smith and Giletti's (1997) values for activation energy (E = 43 kcal/mol) and frequency factor ($D_o = 6.6 \times 10^{-11}$ cm^2/s) was applied. To facilitate the forward modeling process, we have calculated a single weighted mean profile (Fig. 4A) from the eight results (Table 2 [see footnote 1]). In doing so we have normalized measured depths (r) by an assumed effective diffusion radius (r_o) equal to 50 μm. This value was used because it is representative of the average radius of the DH-68-96 grains examined. We emphasize that although our choice of r_o is somewhat arbitrary, results are relatively insensitive to the value employed because D_o is normalized in a similar fashion (i.e., D_o/r_o^2). In addition, while choice of diffusion geometry can significantly affect results at low to intermediate r/r_o values, calculated ages become independent of geometry as r/r_o approaches unity.

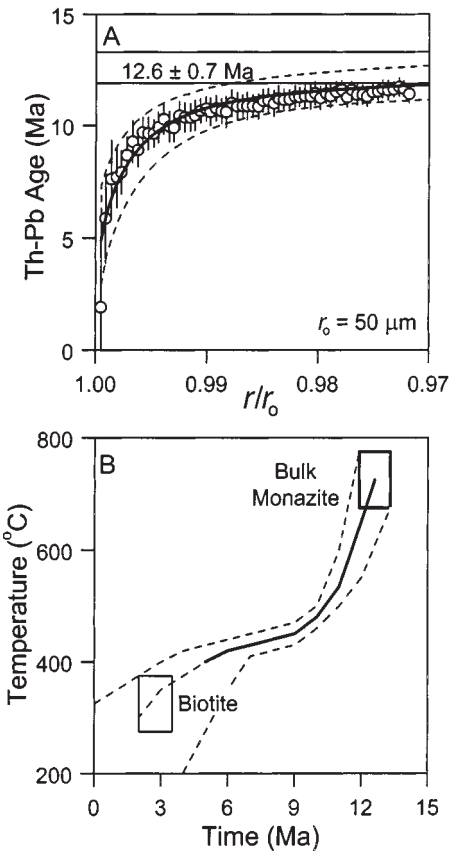

Figure 4. A: Error-weighted mean near surface age variation in DH-68-96 monazite based upon eight individual depth profiles. Horizontal lines represent bulk Th-Pb monazite age (12.6 ± 0.7 Ma) of 24 analyses undertaken following removal of ~10 μm by polishing to expose internal surface. Solid curve is best fit to data and corresponds to temperature-time history shown in B. Dashed curves show how variations in thermal history shown in B affect age profile. B: Best-fit thermal history corresponding to model age profile shown by solid curve in A. Dashed lines in A correspond to cooling history variation depicted in B. $^{40}Ar/^{39}Ar$ biotite ages from Darondi Khola region are from Copeland et al. (1991) and Harrison et al. (1997, 1999), and closure-temperature estimate is from McDougall and Harrison (1988). Monazite bulk closure is calculated from polished DH-68-96 Th-Pb age results, 50 μm diffusion radius, and diffusion parameters of Smith and Giletti (1997).

The form of the profile obtained (Fig. 4A) is consistent with expectations from slow cooling theory (Dodson, 1973). Considering only the possibility of monotonic cooling leads to a highly restricted set of temperature-time histories capable of reproducing the mean age profile. The best-fit solution is shown by the solid curve in Figure 4B. The variation in thermal history defined by the dashed lines in Figure 4B produces the similarly depicted age profiles in Figure 4A. As shown, resolvable differences in depth-profiling results correspond to temperature-time paths that differ only by ±20 °C at temperatures above ~400 °C.

Th-Pb MONAZITE THERMAL HISTORIES: A HIMALAYAN EXAMPLE

The central Himalaya and the Darondi transect in particular have been the focus of numerous petrologic and isotopic studies (e.g., Colchen et al., 1986; Hodges et al., 1988; Copeland et al., 1991; Harrison et al., 1997) and is therefore among the best locations in the Himalaya to test our new method. Attainment of peak (garnet grade) conditions within the shear zone beneath the Main Central thrust at ca. 6–8 Ma has been clearly recorded by analysis of neo-formed monazite (Harrison et al., 1997). Subsequent exhumation of these rocks at 4–2 Ma is recorded by mica closure ages (Copeland et al., 1991). Determining the evolution of the subjacent hanging wall during this interval has been hampered by the fact that conventional thermochronometers tend to record either the earlier amphibolite facies recrystallization (Hodges et al., 1996) or later exhumation (Copeland et al., 1991). However, the high-temperature portion of the retrograde evolution of the hanging wall has been recorded by the distribution of $^{208}Pb^*$ in the rims of older monazites such as those present in DH-68-96. The form of the mean age profile shown in Figure 4A places tight bounds on the temperatures subsequent to 12.8 Ma emplacement of the pegmatite dike. The cooling history that is indicated is reasonably consistent with published geochronologic and pressure-temperature constraints (see Harrison et al., 1998) for the timing of thrust-related exhumation and cooling. However, analysis of individual profiles can lead to somewhat different results (Harrison and Grove, 1998). Nevertheless, the timing of cooling to below 400 °C (Fig. 4B) that is consistently indicated by all profiles (5–3 Ma) is highly compatible with the 4–2 Ma $^{40}Ar/^{39}Ar$ mica ages (Copeland et al., 1991) determined on either side of the Main Central thrust (Fig. 4B).

FINAL REMARKS

The continuous, high-temperature thermal history information afforded by analysis of near-surface monazite Th-Pb age distributions (Fig. 4B) is, to our knowledge, not recoverable by any other means. In this study we elected to deduce the thermochronologic significance of our measurements by analyzing a mean age profile. While variation in measured profiles is anticipated to result from experimental scatter (Fig. 1), it is possible that differences between profiles may reflect additional controls. Among these is the concern that analyzed surfaces may have been damaged during mineral separation and hence may not be representative of the diffusion boundary as it existed in nature. Moreover, the possible existence of metamorphic overgrowths must always be considered. Such problems can potentially be assessed by additional sample characterization, including scanning electron microscope imaging. Regardless, experiments performed with specimen DH-68-96 demonstrate that monazite Th-Pb age depth profiling offers great potential for recovering continuous thermal history data over a temperature range not previously accessible by thermochronometry. Moreover, other applications, such as detecting nannometer-scale igneous and metamorphic overgrowths on accessory minerals (e.g., Zeitler et al., 1989), are equally promising.

ACKNOWLEDGMENTS

This study was supported by grants from the National Science Foundation and U.S. Department of Energy. We thank Chris Coath and Kevin McKeegan for technical assistance in carrying out these measurements and discussions regarding their possible significance. Oscar Lovera assisted us with the diffusion modeling and E. Catlos provided additional information regarding the Main Central thrust. We thank I. Fitzsimons and R. A. Jamieson for helpful reviews.

REFERENCES CITED

Anderson, J. L., Barth, A. P., and Young, E. D., 1988, Mid-crustal Cretaceous roots of Cordilleran metamorphic core complexes: Geology, v. 16, p. 366–369.

Colchen, M., Le Fort, P., and Pêcher, A., 1986, Annapurna-Manaslu-Ganesh Himal notice de la

carte géologique au 1/200,000e (French-English edition): Paris, Centre National de la Recherche Scientifique, 136 p.
Compston, W., Williams, I. S., and Meyer, C., 1984, U-Pb geochronology of zircons from Lunar Breccia 73217 using a sensitive, high mass resolution ion microprobe: Journal of Geophysical Research, v. 89, p. 8525–8534.
Copeland, P., Harrison, T. M., Hodges, K. V., Maréujol, P., LeFort, P., and Pêcher, A., 1991, An early Pliocene thermal perturbation of the Main Central Thrust, Central Nepal: Implications for Himalayan tectonics: Journal of Geophysical Research, v. 96, p. 8475–8500.
Dodson, M. H., 1973, Closure temperature in cooling geochronologic and petrologic systems: Contributions to Mineralogy and Petrology, v. 40, p. 259–274.
Harrison, T. M., and Grove, M., 1998, Monazite Th-Pb age depth profiling: nm-scale thermochonometry: Mineralogical Magazine, v. 62A, p. 573–574.
Harrison, T. M., McKeegan, K. D., and Le Fort, P., 1995, Detection of inherited monazite in the Manaslu leucogranite by $^{208}Pb/^{232}Th$ ion microprobe dating: Crystallization age and tectonic significance: Earth and Planetary Science Letters, v. 133, p. 271–282.
Harrison, T. M., Ryerson, F. J., Le Fort, P., Yin, A., Lovera, O. M., and Catlos, E. J., 1997, A late Miocene–Pliocene origin for the Central Himalayan inverted metamorphism: Earth and Planetary Science Letters, v. 146, p. E1–E8.
Harrison, T. M., Grove, M., Lovera, O. M., and Catlos, E. J., 1998, A model for the origin of Himalayan anatexis and inverted metamorphism: Journal of Geophysical Research, v. 103, p. 27,017–27,032.
Harrison, T. M., Grove, M., McKeegan, K. D., Coath, C. D., Lovera, O. M., and LeFort, P., 1999, Origin and episodic emplacement of the Manaslu intrusive complex: Journal of Petrology, v. 40, p. 3–19.
Hodges, K. V., Le Fort, P., and Pêcher A., 1988, Possible thermal buffering by crustal anatexis in collisional orogens: Thermobarometric evidence from the Nepalese Himalaya: Geology, v. 16, p. 707–710.
Hodges, K. V., Parrish, R. R., and Searle, M. P., 1996, Tectonic evolution of the central Annapurna Range, Nepalese Himalayas: Tectonics, v. 15, p. 1264–1291.
Ireland, T. R., 1995, Ion microprobe mass spectrometry: Advances in Analytical Geochemistry, v. 2, p. 1–118.
Lovera, O. M., Richter, F. M., and Harrison, T. M., 1989, $^{40}Ar/^{39}Ar$ geothermometry for slowly cooled samples having a distribution of diffusion domain sizes: Journal of Geophysical Research, v. 94, p. 17,917–17,935.
McDougall, I., and Harrison, T. M., 1988, Geochronology and thermochronology by the $^{40}Ar/^{39}Ar$ method: New York, Oxford University Press, 212 p.
Montel, J. M., 1993, A model for monazite/melt equilibrium and application to the generation of granitic magmas: Chemical Geology, v. 119, p. 127–146.
Schärer, U., Xu, R. H., and Allegre, C. J., 1986, U-(Th)-Pb systematics and ages of Himalayan leucogranites, South Tibet: Earth and Planetary Science Letters, v. 77, p. 35–48.
Smith, H. A., and Giletti, B. J., 1997, Pb diffusion in monazite: Geochimica et Cosmochimica Acta, v. 61, p. 1047–1055.
Vidal, P., Cocherie, A., and Le Fort, P., 1982, Geochemical investigations of the origin of the Manaslu leucogranite (Himalaya, Nepal): Geochimica et Cosmochimica Acta, v. 46, p. 2279–2292.
Zeitler, P. K., Sutter, J. F., Williams, I. S., Zartman, R., and Tahirkheli, R. A. K., 1989, Geochronology and temperature history of the Nanga Parbat–Haramosh Massif, Pakistan, *in* Malinconico, L. L., Jr., and Lillie, R. J., eds., Tectonics of the Western Himalayas: Geological Society of America Special Paper 232, p. 1–22.

Manuscript received November 13, 1998
Revised manuscript received February 8, 1999
Manuscript accepted February 16, 1999